European Journal of Medicinal Chemistry 50 (2012) 332–343

Contents lists available at SciVerse ScienceDirect

European Journal of Medicinal Chemistry

journal homepage: http://www.elsevier.com/locate/ejmech

Original article

New 4-[(5-arylidene-2-arylimino-4-oxo-3-thiazolidinyl)methyl]benzoic acids active as protein tyrosine phosphatase inhibitors endowed with insulinomimetic effect on mouse C2C12 skeletal muscle cells

Rosaria Ottanà [a,*], Rosanna Maccari [a], Simona Amuso [a], Gerhard Wolber [b], Daniela Schuster [c], Sonja Herdlinger [c], Giampaolo Manao [d], Guido Camici [d,1], Paolo Paoli [d]

[a] Dipartimento Farmaco-chimico, University of Messina, Polo Universitario dell'Annunziata, Viale SS. Annunziata, 98168 Messina, Italy
[b] Freie Universität Berlin, Institut für Pharmazie, Königin-Luisestr., 2+4, 14195 Berlin, Germany
[c] University of Innsbruck, Instiute of Pharmacy and Centre for Molecular Biosciences, Innrain 52, 6020 Innsbruck, Austria
[d] Dipartimento di Scienze Biochimiche, University of Firenze, Vl. Morgagni 50, 50134 Firenze, Italy

ARTICLE INFO

Article history:
Received 2 October 2011
Received in revised form
5 February 2012
Accepted 6 February 2012
Available online 21 February 2012

Keywords:
Enzyme inhibitor
Diabetes mellitus
Obesity
Protein tyrosine phosphatase
Insulinomimetic agent
Molecular docking

ABSTRACT

In pursuing our research targeting the identification of potent inhibitors of PTP1B and LMW-PTP, we have identified new 4-[(5-arylidene-2-arylimino-4-oxo-3-thiazolidinyl)methyl]benzoic acids endowed with interesting in vitro inhibitory profiles. Most compounds proved to be inhibitors of PTP1B and LMW-PTP isoform IF1. The tested inhibitors also showed selectivity towards PTP1B over the closely related TC-PTP. These compounds were found to activate the insulin-mediated signalling on mouse C2C12 skeletal muscle cells by increasing the phosphorylation levels of the insulin receptor and promoting cellular 2-deoxyglucose uptake.

Interestingly, 4-{[5-(4-benzyloxybenzylidene)-2-(4-trifluoromethylphenylimino)-4-oxo-3-thiazolidinyl]methyl}benzoic acid (**7d**), the best in vitro inhibitor of PTP1B and the isoform IF1 of LMW-PTP, provided the highest activation level of the insulin receptor and was found to be endowed with an excellent insulinomimetic effect on the selected cells. This compound therefore represents an interesting lead compound for developing novel PTP1B and LMW-PTP inhibitors which could be achieved by improving both its pharmacological profile and its potentiating effects on insulin signalling.

1. Introduction

Protein tyrosine phosphatases are a superfamily of enzymes involved in crucial cellular signalling mechanisms by controlling the phosphorylation levels of specific tyrosine residues in peptides and proteins which regulate many cellular functions, such as cell proliferation, survival, metabolism, adhesion and migration [1–4].

The balanced and opposing actions of protein tyrosine kinases (PTKs) and protein tyrosine phosphatases (PTPs) regulate the physiological tyrosine phosphorylation levels of proteins. Therefore, defective or inappropriate changes in the activity of either PTKs or PTPs and/or their expression are critically involved in a variety of human diseases including diabetes, obesity and cancer [5–8].

In the past, substantial efforts were made to elucidate the physiopathological role of PTKs which led to the development of drugs targeted at PTKs, such as antireceptor antibodies or small inhibitors, which are currently available in therapeutic regimes for the treatment of cancer [9]. The possible involvement of PTPs in the development of common and serious diseases was understood much later and recently both academic and industrial research groups have shown significant interest in PTPs as potential drug targets [8,10–13].

Among the PTPs so far identified, the cytosolic protein tyrosine phosphatase 1B (PTP1B) was the first phosphatase to be isolated and is therefore the most widely studied enzyme of the family. The role of PTP1B in diabetes and obesity is well-known [5,6,8,13–16].

A large body of experimental data acquired from in vivo studies on humans and PTP1B-knockout mice has identified PTP1B as a major negative regulator of both insulin and leptin signals [14,15,17–19]. Insulin-mediated activation of the insulin receptor

Abbreviations: DM2, type 2 diabetes mellitus; 2-DOG, 2-deoxyglucose; IR, insulin receptor; IRS, insulin receptor substrate; JAK, Janus kinase; LMW-PTP, low molecular weight-protein tyrosine phosphatase; PTK, protein tyrosine kinase; PTP1B, protein tyrosine phosphatase 1B; STAT, signal transducer and activator of transcription; TC-PTP, T-cell protein tyrosine phosphatase.

* Corresponding author. Tel.: +39 90 6766408; fax: +39 90 6766402.
E-mail address: rottana@unime.it (R. Ottanà).
[1] Center of Excellence for Scientific Research DENOTHE, Viale Pieraccini 6, 50139 Firenze, Italy.

0223-5234/$ – see front matter © 2012 Elsevier Masson SAS. All rights reserved.
doi:10.1016/j.ejmech.2012.02.012

(IR), via the autophosphorylation of specific tyrosine residues of the cytoplasmatic portion of the transmembrane IRβ subunits, triggers a cascade of events involved in the regulation of numerous metabolic functions. PTP1B controls the insulin signal through the dephosphorylation of phosphotyrosine (pTyr) residues of not only activated IR but also different downstream substrate proteins such as IRS-1 [5,6,20,21].

It has been shown that the pathological overexpression of PTP1B is involved in the insulin resistance of tissues sensitive to this hormone, including skeletal muscle and liver, thus contributing to the development of type 2 diabetes mellitus (DM2), a cluster of disorders characterised mainly by high blood levels of glucose due to defects in both insulin action and secretion.

The silencing of the PTP1B gene in mice as well as the lack of the enzyme in PTP1B-knockout mice result in increasing insulin sensitivity and resistance to weight gain on a high-fat diet without causing any abnormality in the animals [14,15,22,23]. The administration of PTP1B antisense oligonucleotides to *ob*/*ob* and d*b*/d*b* mice positively modulates downstream events in insulin signalling pathways in targeted tissues [22]. In humans, they increase insulin sensitivity without inducing hypoglycemia [17].

Obesity is an endocrine disorder characterized by leptin resistance. Leptin is a circulating hormone produced primarily by adipose tissue, and it is responsible for energy homeostasis through the control of food intake and energy consumption. Compelling evidence indicates that PTP1B is involved in the regulation of leptin signalling by dephosphorylating the leptin receptor-associated Janus kinase 2 (JAK2). In vivo studies on leptin-deficient mice lacking PTP1B have shown moderate weight gain with normal food intake [5,6,18,19,24,25].

Obesity is also closely linked to the onset of insulin resistance in peripheral tissues. This condition is mediated by adipose-derived cytokines and hormones (among them leptin) that influence insulin action in liver, fat and skeletal muscle [26,27].

Considering the alarming rate and rapid spread of DM2 and obesity in industrialized countries [28], the identification of potent PTP1B inhibitors as drug candidates represents an attractive novel approach to the treatment of these pathologies. Numerous efforts have been thwarted, mainly due to poor selectivity and unfavourable pharmacokinetic profiles of candidates [13,25,29–31]. Of the potent PTP1B inhibitors developed so far, ertiprotafib (Fig. 1) was the first compound to progress to clinical trials for DM2 treatment and the only drug candidate to reach phase 2 clinical trials. However, dose-related adverse effects led to its withdrawal from trials [32]. Currently, trodusquemine (Fig. 1), a selective PTP1B inhibitor, has reached phase 1 clinical trials and shows interesting preclinical results as antidiabetic agent and appetite suppressant [33,34].

Low molecular weight PTP (LMW-PTP) has also been recognized to negatively control insulin signalling by blocking the cascade of events following insulin-mediated receptor activation since it dephosphorylates pTyr specific residues of IR [5,35–38]. LMW-PTP and PTP1B share the same phosphate binding loop structure, although the two enzymes differ as regards tissue specificity. In fact, LMW-PTP knockdown has been found to improve the insulin response in liver and adipose tissue, while PTP1B exerts significant control over the metabolic signalling pathway, especially in liver and skeletal muscle tissue. Thus, the search for dual inhibitors of PTP1B and LMW-PTP could be considered an intriguing challenge for drug discovery destined to treat DM2.

Among PTPs involved in the regulation of IR, the T-cell protein tyrosine phosphatase (TC-PTP) is the PTP that shares with PTP1B the highest sequence identity in catalytic domain (74%) and substantial similarity in the active site [39,40]. TC-PTP is ubiquitously expressed, although is present in higher amount in haematopoietic cells. Gene-targeting studies indicate that TC-PTP null

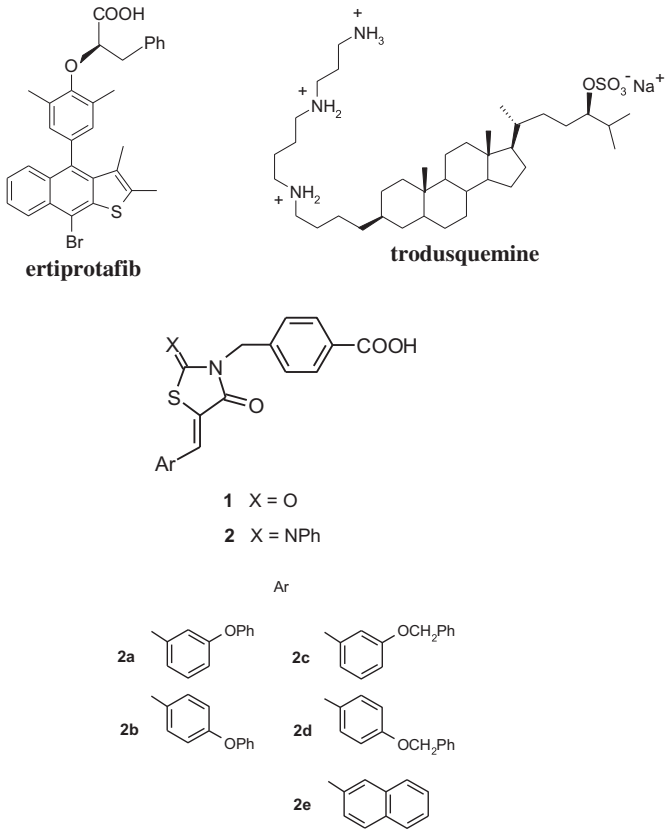

Fig. 1. Chemical structures of some PTP1B inhibitors and selected compounds **2a–e** [55].

mice die by 3–5 weeks of birth as a result of severe anaemia, lymphocytopenia and several inflammatory disorders, while TC-PTP$^{+/-}$ heterozygous mice have normal life expectancy and unaffected immune system [41].

Studies performed with recombinant TC-PTP catalytic domain indicate that the enzyme can dephosphorylate critical pTyr units of IR similarly to PTP1B [42]. Nevertheless, several studies indicate that both enzymes are not redundant PTPs but regulate the IR activation as well as the insulin signalling in a coordinated manner [42,43]. Although TC-PTP and PTP1B possess high similarity in their structure, they show an high degree of substrate selectivity as well as tissue specificity. In vivo studies carried out on liver-specific TC-PTP$^{+/-}$ heterozygous mice underline that the enzyme can reduce both hepatic gluconeogenesis and fasting blood glucose by regulating STAT-3-mediated gluconeogenic gene expression [44].

In obesity, high hypothalamic levels of TC-PTP contribute to leptin resistance condition that is triggered by aberrations in cellular and molecular processes that attenuate the leptin signalling [45].

Taking into account the lethality associated with TC-PTP null mice, its partial inhibition could represent an useful strategy to reduce gluconeogenesis and fasting hyperglicaemia in the control of insulin resistance and obesity [44,46].

The crystal structure of PTP1B provides a valid support for the structure-based design of potent and selective inhibitors [5,16]. The presence of a single preserved catalytic domain characterized by a unique signature motif typifies the PTP family. It represents the phosphate recognition site which accommodates the double negatively charged pTyr moiety of the substrate at physiological pH values. Consequently, in order to mimic the substrate-active-site-directed interactions, most PTP1B competitive inhibitors possess

a high charge density which generally leads to a lack of acceptable cell permeability. The challenge posed for research of effective inhibitors of PTP1B is the identification of small molecules endowed with appropriate physicochemical properties and in vivo efficacy.

PTP1B selectivity represents yet another challenge in the search for potent and safe drug-like molecules for the treatment of diabetes and obesity [29,31,47]. Although the catalytic site is widely conserved throughout the PTP family, it is surrounded by residues that contribute significantly to the recognition of the substrate and these residues are unique for each PTP. A secondary aryl phosphate binding site demarcated by Arg24 and Arg254 has been identified in a PTP1B subpocket adjacent to the active site and represents a good target in order to obtain more selective and potent bidentate inhibitors [5,48–50].

The structure of LMW-PTP is less complex than that of PTP1B. The conserved catalytic pocket is surrounded by the so-called variable loop which contains amino acid residues that determine the selectivity of the two active isoforms of the human enzyme, IF1 and IF2, towards both substrates and inhibitors. The opposite edge of the catalytic cavity is formed by a mobile loop containing the catalytic Asp129 and the residues Tyr131 and Tyr132 that are involved in substrate recognition [51,52].

The search for PTP1B and LMW-PTP inhibitors has been pursued in our laboratory for some years and 4-[(5-arylidene-2,4-dioxo-3-thiazolidinyl)methyl]benzoic acids (**1**, Fig. 1) have been identified as a scaffold of effective bidentate inhibitors of both PTP1B and LMW-PTP. Interesting results have been achieved obtaining potent PTP inhibitors endowed with IC_{50} values at submicromolar levels. They have been shown to act as competitive and reversible PTP inhibitors with significant selectivity for PTP1B and the IF1 isoform of LMW-PTP [53,54].

Molecular docking into the catalytic site of PTP1B indicates that *p*-methylbenzoic acid residue can interact with the catalytically essential Cys215 of the active site acting as a pTyr-mimetic group, while the 5-arylidene moiety binds to the secondary aryl phosphate binding site. Moreover, these studies suggest that the introduction of an additional aromatic ring on position 2 of thiazolidinone moiety may be useful not only to increase lipophilicity, potentially improving bioavailability, but also to enhance binding to Phe182 of the WPD loop situated in proximity to the PTP1B catalytic site. In the catalytically active enzyme, the WPD loop is in an open conformation that, upon the binding of the ligand, undergoes a conformational modification in which Phe182 folds onto the substrate thereby favouring pTyr hydrolysis. In fact, the insertion of a 2-phenylimino moiety in the 4-thiazolidinone scaffold provides 4-[(5-arylidene-2-phenylimino-4-oxo-3-thiazolidinyl)methyl]benzoic acids (**2**, Fig. 1) which have proven to be interesting inhibitors of both PTP1B and the IF1 isoform of LMW-PTP as well as being generally more active than the 2-oxo analogues **1** [54,55].

The SARs so far acquired for this class of compounds clearly indicate that the 5-arylidene moiety plays an important role in the interaction with the target enzymes and, in particular, with the secondary aryl phosphate binding site of PTP1B. An additional aromatic ring in the para or meta position of the 5-benzylidene moiety gives the best enzyme inhibition levels. Phenoxybenzylidene, benzyloxybenzylidene and 2-naphthyl groups in position 5 of the 4-thiazolidinone scaffold are beneficial to the affinity for both PTP1B and LMW-PTP.

On the basis of the SARs so far acquired, further optimization of compounds **2** prompted the design and synthesis of 4-[(5-arylidene-2-arylimino-4-oxo-3-thiazolidinyl)methyl]benzoic acids **7** and **8** (Scheme 1) presented herein in order to ascertain the effect produced by the introduction of substituents on the *para* position of the 2-phenylimino moiety which were selected on the basis of their different electronic and lipophilic nature. As regards the 5-arylidene moiety of compounds **7** and **8**, we inserted the substituents that proved to be beneficial for the enzyme/inhibitor interaction (Scheme 1).

The inhibitory activity of compounds **7** and **8** was investigated against human PTP1B, the two active isoforms of human LMW-PTP (IF1 and IF2) and TC-PTP. Moreover, the effects of the newly

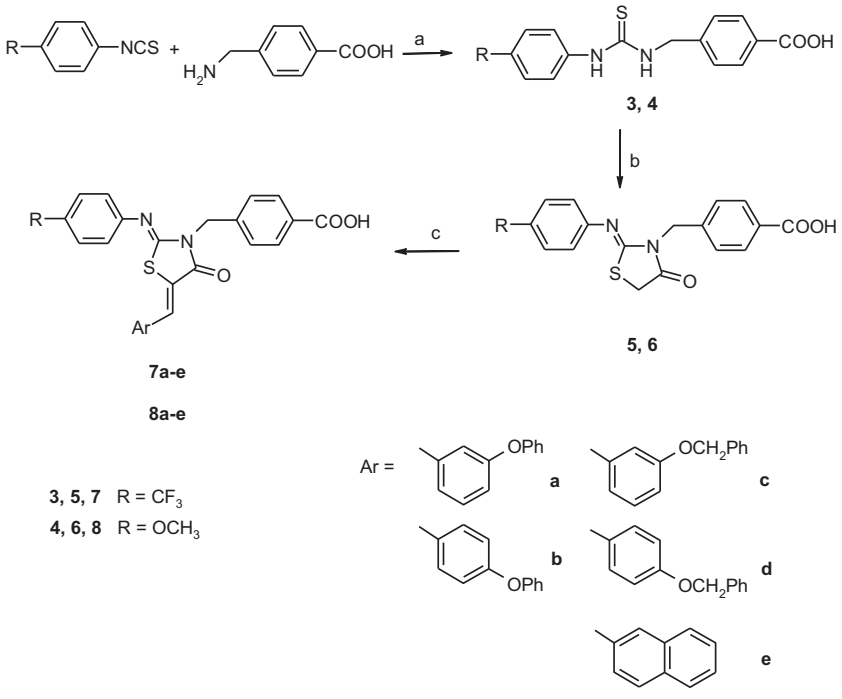

Scheme 1. Reagents and conditions: (a) EtOH, Δ; (b) $ClCH_2COCl$, Et_3N, EtOH, Δ; (c) ArCHO, $C_5H_{11}N$, EtOH, Δ.

synthesized compounds on the activation of the insulin signal pathway were evaluated on mouse C2C12 skeletal muscle cells by measuring the phosphorylation levels of IR as well as the cellular 2-deoxyglucose uptake compared to insulin. In addition, the effect of corresponding 2-phenylimino analogues **2a**–**e** (Fig. 1) [55] on tyrosine phosphorylation of IR was evaluated in the same C2C12 cells.

Molecular docking gave useful insight into the binding mode of inhibitors **7** and **8**.

2. Chemistry

The synthesis of inhibitors **7a**–**e** and **8a**–**e** was carried out according to a previously reported procedure which is depicted in Scheme 1 [54,55].

The intermediate 4-[(3-arylthioureido)methyl]benzoic acids (**3**, **4**) were obtained by the reaction of appropriately substituted arylisothiocyanates with the commercially available 4-(aminomethyl) benzoic acid in refluxing ethanol. The thiazolidinone core structure was synthesized by the reaction of chloroacetyl chloride with thioureas **3**, **4**, under basic conditions, which provided 4-[(2-arylimino-4-oxo-3-thiazolidinyl)methyl]benzoic acids (**5**, **6**) in good yields. In proper experimental conditions, the condensation of thioureas with chloroacetyl chloride can provide two isomers from the two possible ene–thiol intermediates produced by electronic delocalization of the lone pair of the nitrogen atoms linked to the thiocarbonyl group. As already reported, when the reaction was performed in refluxing ethanol starting from N-alkyl-N′-aryl-substituted thioureas only the 2-arylimino isomer, which was more stable than the 2-alkylimino isomer, was obtained [56]. The reaction of suitable benzaldehydes and 2-arylimino-4-thiazolidinones **5**, **6** afforded 4-[(5-arylidene-2-arylimino-4-oxo-3-thiazolidinyl) methyl]benzoic acids (**7a**–**e** and **8a**–**e**, Scheme 1) via Knoevenagel condensation. The reaction time was remarkable reduced when it was performed by microwaves irradiation (80 °C, max 150 psi, max 300 W, 6 h) although the yields were reduced (data not shown). As demonstrated by the X-ray crystallographic analysis of previously synthesized analogues [56,57], all compounds **7** and **8** were obtained solely as Z isomers. In fact, NMR spectra showed in all cases only one set of signals and no isomerization at the C=C exocyclic double bond was subsequently observed [58,59].

The structure of synthesized compounds was assigned on the basis of spectroscopic and analytical data. ^{1}H and ^{13}C NMR spectra were critical for the attribution of structures. In ^{1}H NMR spectra of compounds **5** and **6**, the presence of two singlets at 3.87–3.90 ppm and 5.10 ppm, attributable to the 5-CH_2 and N–CH_2 protons, as well as the typical para-disubstituted systems were diagnostic for the attribution of the structure.

The disappearance of 5-CH_2 signal and the presence of the methylidene proton resonance (7.66–8.16 ppm) proved to be significant for the attribution of the 5-arylidene-2-arylimino-4-thiazolidinone (**7**, **8**) structures.

3. Results and discussion

The newly synthesized 4-[(5-arylidene-2-arylimino-4-oxo-3-thiazolidinyl)methyl]benzoic acids **7a**–**e** and **8a**–**e** were tested for their ability to inhibit the recombinant human PTP1B, the two active isoforms (IF1 and IF2) of human LMW-PTP and TC-PTP (Table 1). *p*-Nitrophenylphosphate was used as substrate.

All compounds proved to be interesting as reversible and competitive inhibitors of PTP1B (Figs. 2 and 3). They were also shown to inhibit both isoforms of LMW-PTP and TC-PTP, showing an overall significant preference for PTP1B.

Table 1
In vitro inhibition activity of compounds **7a**–**e** and **8a**–**e** against human PTP1B, isoforms IF1 and IF2 of human LMW-PTP and TC-PTP.

Compd	IC_{50} (μM)[a]			
	PTP1B	IF1	IF2	TC-PTP
7a	10.4 ± 0.6	13.7 ± 0.7	>150	20.6 ± 3.8
7b	2.2 ± 0.2	7.3 ± 0.2	33.2 ± 1.0	15.6 ± 1.0
7c	5.6 ± 0.1	12.0 ± 0.4	>150	>100
7d	1.4 ± 0.1	4.0 ± 0.1	25.4 ± 0.7	2.2 ± 0.1
7e	2.4 ± 0.1	5.8 ± 0.3	15.2 ± 0.7	20.2 ± 0.8
8a	10.9 ± 0.3	12.0 ± 0.4	21.8 ± 0.4	20.5 ± 0.5
8b	2.5 ± 0.5	11.2 ± 0.3	18.0 ± 0.4	7.1 ± 0.2
8c	5.1 ± 0.9	9.6 ± 0.4	17.5 ± 1.3	11.6 ± 0.4
8d	3.0 ± 0.2	6.4 ± 0.1	9.1 ± 0.2	9.5 ± 0.5
8e	9.0 ± 0.3	11.6 ± 0.3	11.7 ± 0.4	27.0 ± 0.9

[a] IC_{50} values were determined by regression analyses and expressed as means ± SE of three replicates.

Indeed, both 2-(4-trifluoromethylphenylimino) substituted derivatives **7a**–**e** and 2-(4-methoxyphenylimino) analogues **8a**–**e** exhibited appreciable inhibitory effects against PTP1B with low micromolar IC_{50} values. These results suggest that in this series of inhibitors the trifluoromethyl group on the 2-arylimino moiety is generally more favourable than the methoxy group resulting in higher affinity for the enzyme. In fact, compounds **7a** and **7b** were slightly more active than analogues **8a** and **8b**, while **7d** and **7e** were two to threefold more effective than **8d** and **8e**.

Among the 5-arylidene-2,4-thiazolidinediones **1** and 2-phenylimino analogues **2** previously reported to be inhibitors of both PTP1B and LMW-PTP, the substituents on the 5-arylidene moiety play a determining role in the interaction with PTP1B and correlated enzymes [53–55]. The phenoxy and benzyloxy groups on the 5-arylidene moiety bring about enhanced PTP1B inhibitory activity compared to non-aromatic substituents, improving the stability of the enzyme/inhibitor complex, especially when inserted in the para position [53,55]. The inhibitory ability of compounds **7** and **8** against selected PTPs proved to be in close agreement with the structure–activity relationships already acquired for this class of inhibitors. In this new series, the insertion of the 4-phenoxy (**7b**

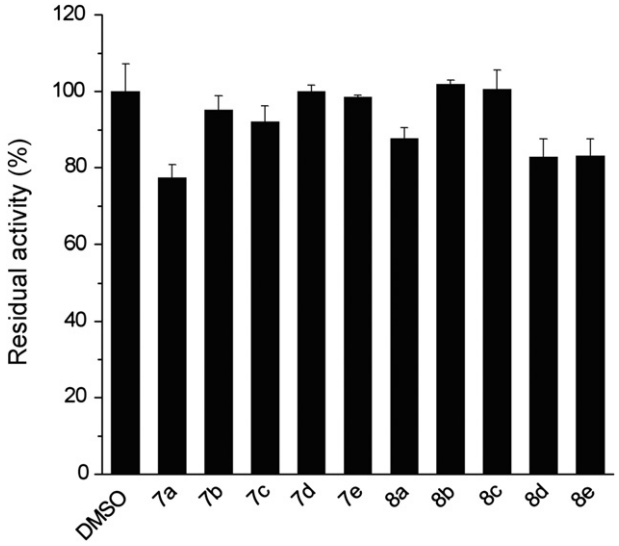

Fig. 2. Inhibition reversibility assay of compounds **7a**–**e** and **8a**–**e**. Aliquots of PTP1B were incubated in the presence of at least 25-fold molar excess of each compound for 1 h at 37 °C. Then, the enzyme was diluted 200-fold with the assay solution to measure the residual activity (37 °C, 5 mM *p*NPP). Control experiments were carried out adding DMSO. Data represent the mean ± SE of three replicates.

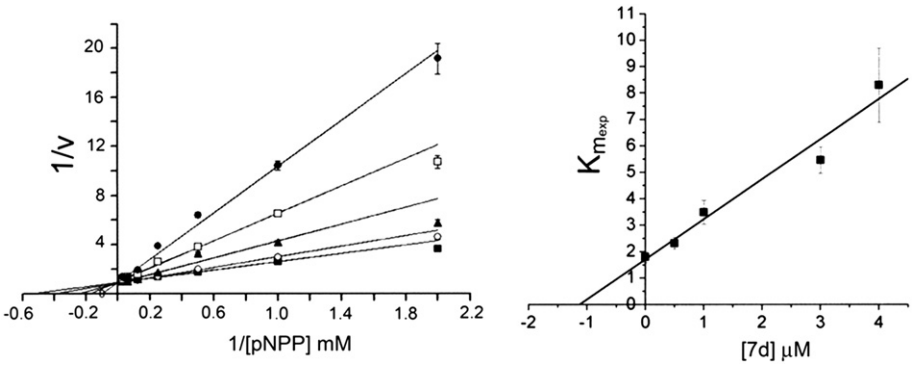

Fig. 3. Left panel: Lineweaver–Burk plots at differing concentrations of **7d**, the best inhibitor of PTP1B. The used concentrations of inhibitor were: 0 mM (●); 0.5 mM (○); 1.0 mM (▲); 3 mM (□); 4 mM (◆). Right panel: re-plot of the apparent K_m values measured at differing concentrations of 7 d against the concentrations of the inhibitor. Data represent the mean ± SE of three replicates.

and **8b**) and 4-benzyloxy (**7d** and **8d**) groups provided more potent PTP1B inhibitors than the corresponding 3-phenoxy (**7a** and **8a**) and 3-benzyloxy (**7c** and **8c**) substituted derivatives, determining a gain in potency which was significant for **7b** (fivefold), **7d** and **8b** (fourfold) compared to the meta substituted isomers (Table 1).

With the same substituent on the 2-phenylimino group, the benzyloxy group on the 5-arylidene moiety was found to exert a generally more favourable effect than the phenoxy one for interactions with PTP1B regardless of its position on the benzene ring.

Compound **7d**, the best PTP1B inhibitor of this series of compounds, proved to be up to eightfold more effective than the other tested compounds, showing a K_i value of 1.2 ± 0.2 μM.

Compounds **7e** and **8e**, 5-naphtalen-2-ylmethylidene substituted derivatives, also exhibited good affinity for PTP1B. Once again, 4-trifluoromethylphenylimino derivative **7e** was more active against PTP1B than the corresponding 4-methoxyphenylimino analogue **8e**.

The comparison between the in vitro activity of derivatives **7a**–**e** and **8a**–**e** and the previously reported corresponding 2-phenylimino analogues (**2a**–**e**, Fig. 1) [55] highlighted that the introduction of the selected substituents in para position of the 2-phenylimino moiety generally brought about a clear-cut increase of IC_{50} values against all tested PTPs, regardless of the electronic nature of the substituents; however they maintained a good inhibitory ability against PTP1B. This was particularly evident for compounds **7a** and **8a** (IC_{50} 10.4 and 10.9 μM, respectively), which proved to be fivefold less active than the corresponding 2-phenylimino analogue **2a** (Fig. 1, IC_{50} 1.9 μM) [55]. However, the most effective inhibitor of the new series, compound **7d**, yielded an interesting IC_{50} value (1.4 μM) very close to that of the corresponding 2-phenylimino **2d** analogue (Fig. 1, IC_{50} 1.1 μM) [55]. The detrimental effect resulting from the introduction of CF_3 and OCH_3 groups could be attributable to a steric hindrance that prevented effective interactions with the residues of the loops surrounding the PTP1B catalytic site. On the basis of these results, it seems plausible to suggest that the introduction of substituents on the 2-phenylimino group, although endowed with different electronic or lipophilic features, might hinder inhibitors from making beneficial contacts with the amino acid residues flanking the catalytic site of the enzyme.

The inhibition profiles of the tested compounds towards LMW-PTP isoforms IF1 and IF2 are reported in Table 1. All tested compounds were shown to inhibit both isoenzymes, without, however, achieving the inhibitory levels against PTP1B. Like previously reported derivatives **1** and **2**, 2-arylimino-5-arylidene-4-thiazolidinones **7** and, to a lesser extent, **8** proved to be preferential inhibitors of the IF1 isoform achieving from threefold to more than tenfold higher inhibitory activity levels towards IF1 over isoform IF2. The ascertained preferential inhibition of IF1 isoform over IF2 of this class of inhibitors (**1**, **2**, **7** and **8**) can be considered favourable for the control of insulin resistance, since the isoenzyme IF1 appears to be the main LMW-PTP isoform associated with hyperglycemia in diabetic patients [60].

Out of both compounds **7** and **8**, the benzyloxy group, in either the *meta* or *para* position of the 5-arylidene moiety, proved to be the most favourable substituent, also for the interaction with LMW-PTP.

Within the same series of compounds, it can be inferred that the para position is once again the most favourable as **7b**, **7d** and **8b**, **8d** were more active than **7a**, **7c** and **8a**, **8c** towards both isoforms of LMW-PTP.

Among the 5-naphtalen-2-ylmethylidene substituted compounds, the analogous *p*-trifluoromethylimino derivative **7e** showed clear selectivity towards the IF1 isoform, while **8e** did not determine any difference in the levels of inhibitory ability of both isoenzymes.

The inhibitory effects of compounds **7** and **8** towards TC-PTP are reported in Table 1. Compounds **7** and **8** were shown to be inhibitors of TC-PTP, even though none of compounds achieved the interesting levels of affinity towards PTP1B. Overall, the substituent on 2-arylimino moiety was not critical since compounds **7** (p-trifluorophenylimino substituted) were generally as active as compounds **8** (*p*-methoxyphenylimino substituted).

In both series of inhibitors (compounds **7** and **8**) the presence of the selected substituents on the *para* position of 5-benzylidene group (**7b**, **d** and **8b**, **d**) resulted to be favourable in comparison with the *meta* substitution (**7a**, **c** and **8a**, **c**). Within trifluoromethylphenylimino substituted derivatives, compound **7d**, bearing a *p*-benzyloxy group on the 5-phenylidene moiety, proved to be the best inhibitor of TC-PTP which resulted to be about sevenfold more active than 4-phenoxy analogous **7b**. Out of compounds **8**, the introduction of *p*-benzyloxy and *p*-phenoxy groups on 5-phenylidene moiety provided inhibitors endowed with comparable inhibitory activity levels towards TC-PTP. The introduction of 5-naphtalen-2-ylmethylidene group (compounds **7e** and **8e**) proved to be detrimental for the interaction with TC-PTP by determining a clear-cut decrease from threefold (**8e**) to tenfold (**7e**) of inhibitory ability towards the enzyme. In all cases, the tested compounds showed to be from twice to more than twenty-fold selective towards PTP1B over TC-PTP. Taking into account the high similarity between the catalytic domains of both enzymes, the significant selectivity of *p*-trifluoromethylphenylimino substituted compounds **7b**, **7c** and **7e** can be considered an appreciable goal in

the development of new agents for the treatment of obesity and DM2. In fact, the inhibitory profile of these compounds can be considered a favourable feature since the partial inhibition of TC-PTP can contribute to the control of insulin resistance without affecting immune system [44,46].

The discovery of pharmaceutically useful PTP1B inhibitors for the treatment of insulin resistance in obesity and DM2 remains a great challenge to develop small pTyr-mimetic molecules into orally available drugs endowed with appropriate physicochemical properties and in vivo effectiveness.

Therefore, in order to evaluate the efficacy of all tested compounds in cells, in vitro inhibitors **7**, **8** and, for comparison, compounds **2a**–**e** were assayed on cultures of differentiated mouse C2C12 myotubes which constitutively express both PTP1B and IR.

Even at the highest dose of 25 μM, compounds **7** and **8**, did not interfere with the viability of cells, which maintained their ability to reduce the MTT to formazan (Fig. 4).

Incubating the tested compounds (25 μM final dose) with C2C12 cells highlighted their ability to influence IR activation (Fig. 5). All compounds **7** and **8**, except derivative **8d**, induced a notable increase in tyrosine phosphorylation levels of the IRβ subunits compared to controls. Although it was not possible to draw clear SARs, it is worth underlining that most compounds (**7c**–**e**, **8a**–**c**) at 25 μM concentration in the medium were able to activate the IR to a similar extent as that produced by insulin (10 nM). Interestingly, compound **7d**, the best inhibitor of both PTP1B and the IF1 isoform of LMW-PTP, induced the highest degree of IR phosphorylation. Moreover, all compounds **7** and **8**, with the exception of **8d**, were shown to be more effective than corresponding 2-phenylimino substituted compounds **2**, even when these latter were tested at higher dose (see supplementary material). Interestingly, these results indicated that the introduction of the selected substituents on the *para* position of the 2-phenylimino moiety was shown to enhance the tyrosine phosphorylation of the IR, although compounds **7** and **8** resulted to be less potent PTP1B inhibitors than analogues **2**.

Compounds **7** and **8** (25 μM final dose) were also incubated in C2C12 cell cultures for 90 min in order to evaluate the cellular uptake of 2-deoxyglucose (2-DOG). Compounds **7a**, **c**–**e** were shown to increase intracellular 2-DOG uptake significantly whereas analogues **8** did not elicit any effect (Fig. 6). The 2-DOG uptake

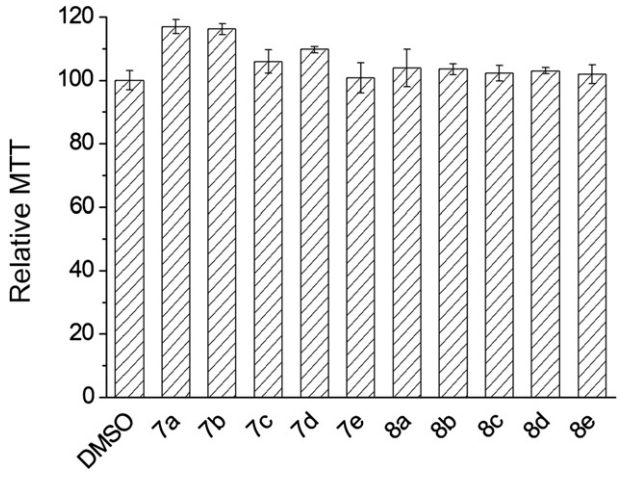

Fig. 4. MTT responses in differentiated C2C12 cell cultures treated with compounds **7a**–**e** and **8a**–**e** (25 μM final concentration in the culture medium). The MTT assay was used to evaluate toxicity of the tested compounds after 2 h of exposure. Each point is the mean absorbance at 570 nm converted to percentage of control values (DMSO). Data represent the mean ± SE of three replicates.

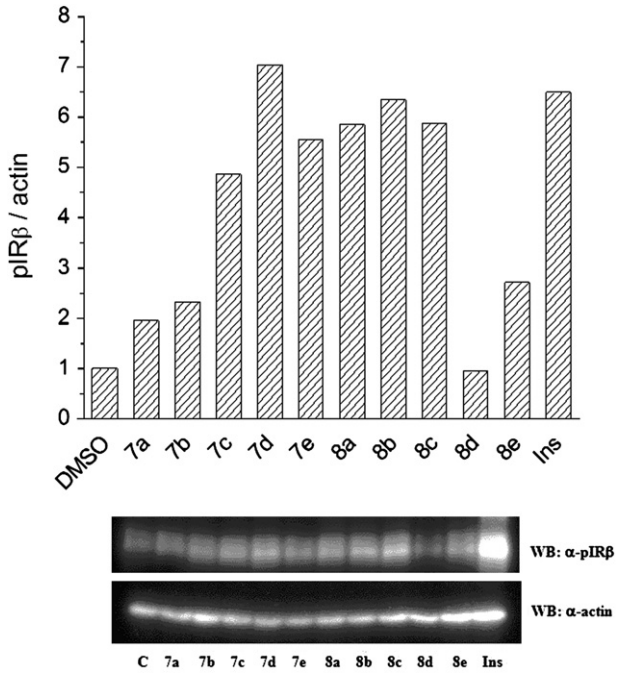

Fig. 5. Effect of compounds **7a**–**e** and **8a**–**e** and insulin on tyrosine phosphorylation of IR in differentiated C2C12 cells. Cells were incubated at 37 °C with the compounds (25 μM final concentration) for 90 min as well as with insulin (10 nM final concentration) for 30 min. Proteins of the cell lysates were separated by SDS-PAGE and then transferred to polyvinylidene membranes, which were probed with anti-phospho–insulin receptor β-subunit (α-pIRβ) antibodies. Then membrane was reprobed with anti-actin (α-actin) antibodies. Data are representative of at least three separate experiments. Top panel, data normalized against actin. Bottom panel: western blotting.

levels determined by compounds **7a**, **c**–**e** at 25 μM concentration in the medium were comparable to that produced by insulin (10 nM). These results suggest that the compounds are cell-permeable and able to strengthen insulin signalling by interfering with downstream components of the insulin signal cascade.

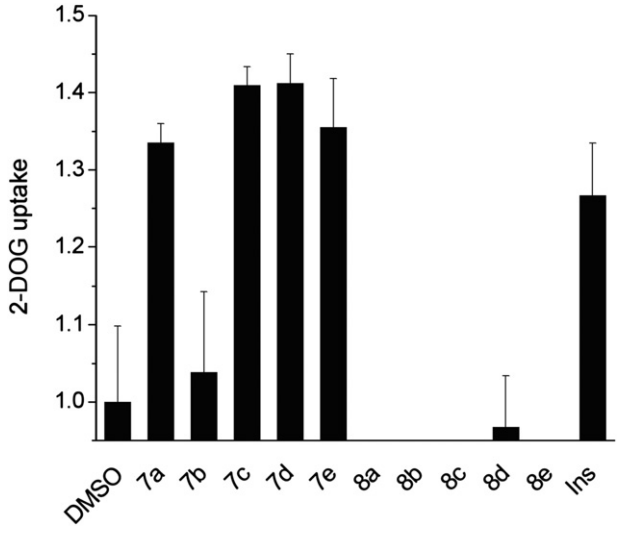

Fig. 6. 2-Deoxyglucose (2-DOG) uptake in C2C12 myotubes. Cells were serum-starved for 20 h and then treated with **7a**–**e** and **8a**–**e** (25 μM final concentration), or DMSO for 90 min, or insulin (10 nM) for 30 min. Subsequently, 0.1 μCi 2-deoxy-D-1,2-[^{3}H-glucose] in Ringer–Hepes was added to each well, and glucose uptake was allowed at 37 °C for 15 min. Aliquots of the lysates were counted in a liquid scintillation counter. Data represent the mean ± SE of three replicates, and were normalized against protein concentration.

The observed structure–activity relationships indicate that the trifluoromethylphenylimino group (**7**) can significantly contribute to promoting the insulinomimetic activity and bioavailability of this class of compounds, probably due to the greater lipophilicity of the CF_3 group compared to the methoxy group (**8**).

In order to gain insight into the interaction of inhibitors with the enzyme binding site molecular docking studies were performed. PDB [61] entry 2QBS [62] was selected as template for human PTP1B. 5PNT [63] and 1XWW [64] were selected as structures for human LMW-PTP IF1 and IF2, respectively. The selected protein structures were processed with CCDCs software GOLD version 5 [65] for docking experiments. After docking, structures were minimized in the binding site using LigandScout's [66] MMFF94 implementation, and prioritized using a 3D pharmacophore model that explains the most plausible docking poses. The conformations obtained were all oriented with the carboxylic acid towards the catalytic centre. For compounds **7**, the trifluoromethylphenylimino moiety is oriented towards the solvent, while the phenyl ring of the residue of *p*-methylbenzoic acid shows a π-stacking interaction with Phe182 located in the WPD loop. However, the trifluoromethyl moiety of compounds **7b**, **7d** and **7e** is oriented in such a way that an electrostatic interaction of one of the fluorine atoms with Arg24 becomes possible (Figs. 7 and 8), which may explain the higher activity of those compounds.

For compounds **8**, we observed poses where the methoxy moiety either points to the side of the WPD loop or towards the solvent (Fig. 7). The phenyl ring in the 4-phenoxybenzylidene moiety of compound **8b** allows for an orientation towards Arg254 enabling a cation-π interaction, while in **8d** the benzyl ring reaches out to the hydrophobic Ala27, which might provide an explanation for the higher activities of these two compounds in series **8** (Fig. 7).

Overall, the binding of compounds **7** and **8** is dominated by hydrophobic interactions involving residues Tyr46, Phe182, Ile219 and Met258 (Fig. 8 shows compound **7e** as a representative example in detail).

The lower activity of the tested compounds towards IF1 and IF2 may be explained by the smaller and less deep binding pockets compared to human PTP1B. For IF1, an additional weak hydrogen bond with Tyr49 could be proposed with either the ether oxygen of the 5-arylidene moiety (**7a**–**d** and **8a**–**d**) or the methoxy oxygen of the 2-arylimino moiety. In Fig. 9, compound **7d** docked into LMW-PTP isoform IF1 is reported as representative of this binding mode. In this pose, the carboxylate group of the *p*-methylbenzoic acid moiety potentially interacts with residues of the catalytic site through charge transfer (Arg18) and a network of hydrogen bonds (Ile16, Cys17 and Arg18). In addition, a weak hydrogen bond of the benzyloxy oxygen atom with Tyr49 is observed. For IF2, no plausible docking poses could be found for compounds **7c** and **7d**. The 3-benzyloxybenzylidene moiety of **7c** is trapped between the trifluoromethyl group and Trp49, and therefore the compound would be forced in a highly strained conformation upon putative binding, which might account for the inactivity of compound towards IF2 (data not shown).

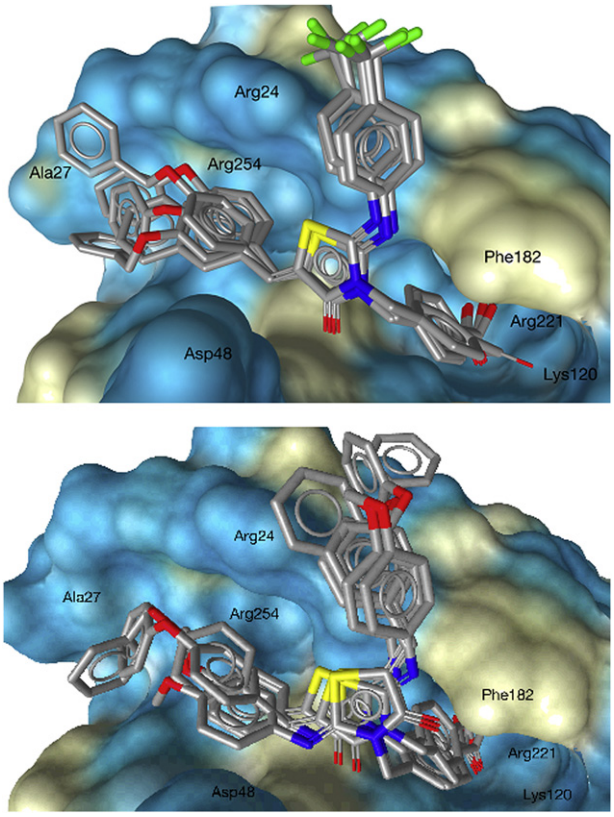

Fig. 7. Compounds **7a**–**e** (top) and **8a**–**e** (bottom) docked into human PTP1B (PDB entry 2QBS). Molecular surface shows hydrophobic regions in yellow, hydrophilic regions in blue. Visualization was performed with LigandScout 3.02 [66]. (For interpretation of the references to colour in this figure legend, the reader is referred to the web version of this article.)

4. Conclusions

In continuing the search for inhibitors of PTP1B and LMW-PTP through targeted structural modifications of previously reported analogues, new 5-arylidene-2-aryilimino-4-thiazolidinones, highly active inhibitors of both PTP1B and the isoform IF1 of LMW-PTP, were identified. In all cases, the tested compounds showed to be from moderately to significantly selective towards PTP1B over closely related TC-PTP.

Moreover, most tested compounds were endowed with cellular activity. They were able to activate the IR on mouse C2C12 skeletal muscle cells since their addition to the culture medium brought about an increase in the level of IRβ tyrosine phosphorylation. Interestingly, compounds **7c**–**e** and **8a**–**c** induced IR activation levels similar to those of insulin. In addition, compounds **7** and **8** resulted to enhance IR tyrosine phosphorylation to a greater extent than analogues **2**, indicating that the introduction of the selected substituents on the *para* position of the 2-phenylimino moiety can favour the effect of these compounds on the IR activation.

At the tested doses, compounds **7a**, **c**–**e** were also able to promote the intracellular uptake of 2-DOG to an extent that is comparable to that induced by insulin, therefore they can be considered insulinomimetic agents. Overall, these results indicate that they are able to strengthen the insulin signal likely by inhibiting PTP1B activity; this causes the enhancement of insulin receptor phosphorylation and thus activates other downstream components of the insulin signalling pathway including those of the final pathway that induce the movement of GLUT4 vesicles to the plasma membrane. However, we found that compounds **8a**–**c**, **e** were able to stimulate IR phosphorylation but were unable to increase cellular 2-DOG uptake. These findings suggest that they not only inhibit PTP1B but may also negatively interfere with downstream components of the insulin signal cascade.

As regards structure–activity relationships, 2-(4-trifluoromethylphenylinimo) substituted analogues **7** proved to be

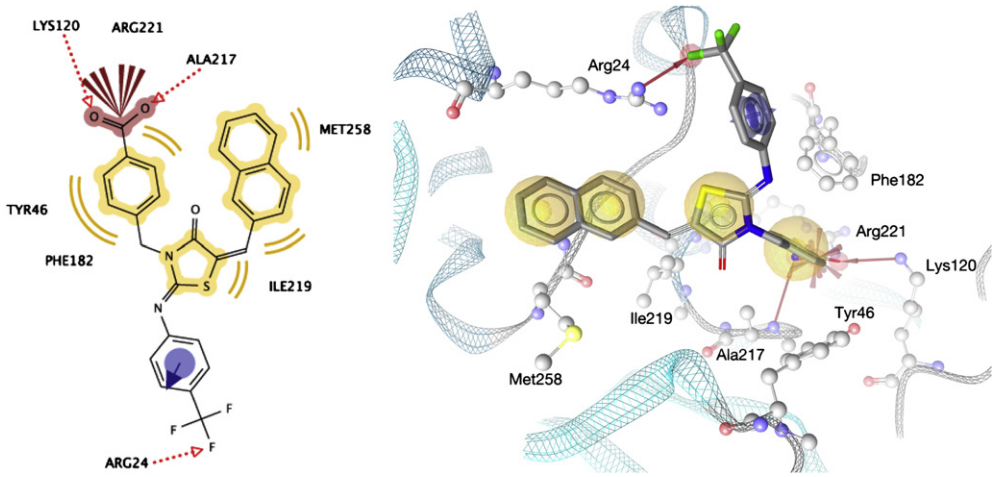

Fig. 8. Compound **7e** docked into human PTP1B (PDB entry 2QBS). Interactions were automatically detected and visualized in 2D (left) and 3D (right) by LigandScout [66]. Yellow spheres indicate lipophilic regions, pink disks cation-π interactions, and red arrows hydrogen bonds or electrostatic fluorine-donor interactions. (For interpretation of the references to colour in this figure legend, the reader is referred to the web version of this article.)

endowed with excellent insulinomimetic effect in mouse skeletal muscle cells, despite the fact that the insertion of a substituent in the para position of the 2-phenylimino ring was found to be either indifferent or unfavourable for the in vitro inhibition of PTP1B and LMW-PTP.

Of note among these is compound **7d**, the best inhibitor of both PTP1B and the isoform IF1 of LMW-PTP, which determined the highest degree of phosphorylation of IR and also promoted a high level of glucose uptake. In addition, it showed a modest selectivity towards PTP1B over TC-PTP.

It is also worth noting that, out of the tested compounds, **7c** is the most selective inhibitor of PTP1B and LMW-PTP IF1 isoform over both IF2 and TC-PTP and is endowed with a potent insulinomimetic activity on C2C12 cells. Overall, a relatively low inhibition of TC-PTP associated with PTP1B inhibition is considered to be useful to cooperate in the improvement of insulin resistance in DM2 and obesity without interfering with haematopoietic and immune functions [44,46]. Compounds **7**, which are endowed of promising activity profiles, can therefore be recruited as lead compounds for the design of new drugs for the treatment of DM2 and obesity.

5. Experimental section

5.1. Chemistry

Melting points were recorded on a Kofler hot-stage apparatus and are uncorrected. Reactions were monitored by thin layer chromatography (TLC) on Merck 0.2 mm precoated silica gel plates aluminium sheets (60 F 254 Merck) and visualized by irradiation with a UV lamp.

Elemental analyses (C, H, N) were performed on a C. Erba mod. 1106 elem. Analyzer and were within $\pm$0.4% of the theoretical values. ^{1}H and ^{13}C NMR spectra were recorded on a Varian 300 magnetic resonance spectrometer (300 MHz for ^{1}H and 75 MHz for ^{13}C). Chemical shifts are given in δ units (ppm) relative to internal standard Me_4Si in $CDCl_3$ or DMSO-d_6 used as solvents. Coupling constants (J) are given in hertz (Hz). ^{13}C NMR spectra were determined by Attached Proton Test (APT) experiments and the resonances were always attributed by proton–carbon heteronuclear chemical shift correlation. Reactions under microwaves were performed in a microwave oven Discover (CEM). Unless stated otherwise, all materials were obtained from commercial suppliers and

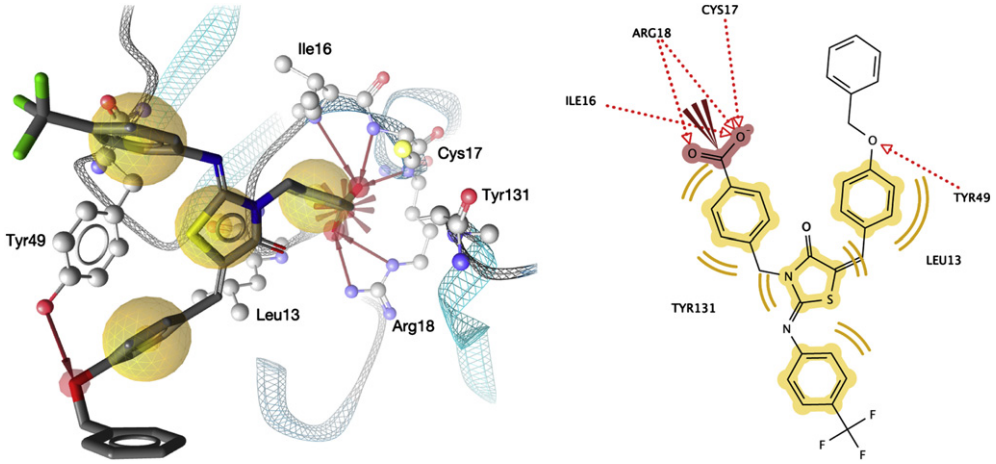

Fig. 9. Complementary chemical features of compound **7d** docked into LMW-PTP isoform IF1 (PDB entry 5PNT) analyzed in 3D (left) and 2D (right) using LigandScout [66]. Yellow spheres indicate lipophilic regions, red arrows hydrogen bond acceptors, and red rays the ionic interaction if the carboxylic acid moiety with Arg18. (For interpretation of the references to colour in this figure legend, the reader is referred to the web version of this article.)

used without further purification. All tested compounds possessed a purity of at least 95% as verified by elemental analyses by comparison with the theoretical values.

*5.1.1. General procedure for the synthesis of 4-[(3-arylthioureido) methyl]benzoic acids (**3**, **4**)*

A mixture of appropriate arylisothiocyanate (2.6 mmol) and 4-(aminomethyl)benzoic acid (0.51 g, 3.4 mmol) in ethanol (50 ml) was refluxed for 24 h. The solvent was evaporated under vacuo and the solid residue was crystallized from methanol providing reaction products **3** and **4**.

*5.1.1.1. 4-{[3-(4-Trifluoromethylphenyl)thioureido]methyl}benzoic acid (**3**).* Yield 74%; mp 265–268 °C; ^{1}H NMR (DMSO-d_6): δ 4.83 (d, J = 5.4 Hz, 2H, NCH_2); 7.36 (m, 2H, arom); 7.43–7.88 (m, 4H, arom); 7.91 (m, 2H, arom); 8.66 (brs, 1H, N*H*CH_2); 10.15 (brs, 1H, NH); 11.38 (brs, 1H, COOH). Anal. calcd for $C_{16}H_{13}F_3N_2O_2S$: C, 54.23; H, 3.70; N, 7.91. Found: C, 54.01; H, 3.55; N, 7.79.

*5.1.1.2. 4-{[3-(4-Methoxyphenyl)thioureido]methyl}benzoic acid (**4**).* Yield 93%; mp 245–248 °C; ^{1}H NMR ($CDCl_3$): δ 3.67 (s, 3H, OCH_3); 4.78 (s, 2H, NCH_2); 6.78 (m, 2H, arom); 6.86 (brs, 1H, NH); 7.11 (m, 2H, arom); 7.25 (m, 2H, arom); 7.87 (m, 2H, arom); 8.54 (s, 1H, N*H*CH_2); 9.98 (s, 1H, COOH); Anal. calcd for $C_{16}H_{16}N_2O_3S$: C, 60.74; H, 5.10; N, 8.85. Found: C, 60.55; H, 5.21; N, 8.73.

*5.1.2. General method for the synthesis of 4-[(2-arylimino-4-oxo-3-thiazolidinyl)methyl]benzoic acids (**5**, **6**)*

A mixture of appropriate 4-[(3-arylthioureido)methyl]benzoic acid (**3**, **4**) (1.7 mmol) and triethylamine (0.52 g, 5.1 mmol) in ethanol (50 ml) was maintained at reflux for 30 min. After cooling to room temperature, a solution of chloroacetyl chloride (0.28 g, 2.5 mmol) in ethanol (10 ml) was added and the mixture was refluxed for 24 h. After evaporation of the solvent under reduced pressure, the crude solid was dissolved in $CHCl_3$ and the solution was washed with water. The crude mixture was purified by chromatography on silica gel column (diethyl ether/*n*-hexane, 6/4). The crystallization from methanol provided pure compounds **5** and **6**.

*5.1.2.1. 4-{[2-(4-Trifluoromethylphenylimino)-4-oxo-3-thiazolidinyl] methyl}benzoic acid (**5**).* Yield 76%; yellow oil; ^{1}H NMR ($CDCl_3$): δ 3.91 (s, 2H, 5-CH_2); 5.10 (s, 2H, NCH_2); 7.02 (m, 2H, arom); 7.56–7.61 (m, 4H, arom); 8.09 (m, 2H, arom); Anal. calcd for $C_{18}H_{13}F_3N_2O_3S$: C, 54.82; H, 3.32; N, 7.10. Found: C, 54.52; H, 3.43; N, 6.94.

*5.1.2.2. 4-{[2-(4-Methoxyphenylimino)-4-oxo-3-thiazolidinyl]methyl} benzoic acid (**6**).* Yield 77%; mp 157–160 °C; ^{1}H NMR ($CDCl_3$): δ 3.81 (s, 3H, OCH_3); 3.87 (s, 2H, 5-CH_2); 5.10 (s, 2H, NCH_2); 6.90 (m, 4H, arom); 7.58 (m, 2H, arom); 8.07 (m, 2H, arom); 9.98 (s, 1H, COOH); Anal. Calcd for $C_{18}H_{16}N_2O_4S$: C, 60.66; H, 4.53; N, 7.86. Found: C, 60.49; H, 4.61; N, 7.76.

*5.1.3. General method for the synthesis of 4-[(5-arylidene-2-arylimino-4-oxo-3-thiazolidinyl)methyl]benzoic acids (**7a**–**e**, **8a**–**e**)*

A mixture of appropriate 4-[(2-arylimino-4-oxo-3-thiazolidinyl) methyl]benzoic acids (**5**, **6**) (1.5 mmol), opportune aldehyde (1.5 mmol) and piperidine (0.26 g, 3 mmol) in ethanol (50 ml) was refluxed until the starting materials disappeared (72–96 h, TLC analysis). The solution was poured in water acidified with glacial acetic acid. The crude solid was washed with H_2O, dried and purified by chromatography on silica gel column (diethyl ether/*n*-hexane, 8/2). The crystallization from methanol provided pure acids **7** and **8**.

*5.1.3.1. 4-{[2-(Trifluoromethylphenylimino)-4-oxo-5-(3-phenoxybenzylidene)-3-thiazolidinyl]methyl}benzoic acid (**7a**).* Yield 27%; mp 214–216 °C; ^{1}H NMR ($CDCl_3$): δ 5.22 (s, 2H, NCH_2); 6.99–7.04 (m, 3H, arom); 7.08–7.16 (m, 2H, arom); 7.29–7.41 (m, 6H, arom); 7.55–7.66 (m, 4H, arom); 7.75 (s, 1H, CH methylidene); 8.03 (m, 2H, arom); Anal. calcd for $C_{31}H_{21}F_3N_2O_4S$: C, 64.80 H, 3.68; N, 4.88. Found: C, 64.69; H, 3.51; N, 4.73.

*5.1.3.2. 4-{[2-(4-Trifluoromethylphenylimino)-4-oxo-5-(4-phenoxybenzylidene)-3-thiazolidinyl]methyl}benzoic acid (**7b**).* Yield 36%; mp 256–258 °C; ^{1}H NMR ($CDCl_3$): δ 5.24 (s, 2H, NCH_2); 6.99–7.07 (m, 6H, arom); 7.19 (m, 1H, arom); 7.36–7.43 (m, 4H, arom); 7.61–7.65 (m, 4H, arom); 7.78 (s, 1H, CH methylidene); 8.08 (m, 2H, arom); Anal. calcd for $C_{31}H_{21}F_3N_2O_4S$: C, 64.80; H, 3.68; N, 4.88. Found: C, 64.62; H, 3.39; N, 4.57.

*5.1.3.3. 4-{[5-(3-Benzyloxybenzylidene)-2-(4-trifluoromethylphenylimino)-4-oxo-3-thiazolidinyl]methyl}benzoic acid (**7c**).* Yield 37%; 242–244 °C (dec.); ^{1}H NMR (DMSO-d_6): δ 5.11 (s, 2H, NCH_2); 5.13 (s, 2H, OCH_2); 7.10 (m, 2H, arom); 7.21 (m, 2H, arom); 7.30–7.40 (m, 8H, arom); 7.77–7.87 (m, 6H, arom and CH methylidene); Anal. calcd for $C_{32}H_{23}F_3N_2O_4S$: C, 65.30; H, 3.94; N, 4.76. Found: C, 65.21; H, 3.79; N, 4.63.

*5.1.3.4. 4-{[5-(4-Benzyloxybenzylidene)-2-(4-trifluoromethylphenylimino)-4-oxo-3-thiazolidinyl]methyl}benzoic acid (**7d**).* Yield 62%; mp 278–280 °C; ^{1}H NMR ($CDCl_3$): δ 5.01 (s, 2H, NCH_2); 5.11 (s, 2H, OCH_2); 6.90–6.98 (m, 4H, arom); 7.29–7.55 (m, 11H, arom); 7.66 (s, 1H, CH methylidene); 7.93 (m, 2H, arom); Anal. calcd for $C_{32}H_{23}F_3N_2O_4S$: C, 65.30; H, 3.94; N, 4.76. Found: C, 65.19; H, 3.71; N, 4.59.

*5.1.3.5. 4-{[2-(4-Trifluoromethylphenylimino)-5-(naphthalen-2-ylmethylidene)-4-oxo-3-thiazolidinyl] methyl]}benzoic acid (**7e**).* Yield 35%; mp dec. starting from 240 °C; ^{1}H NMR (DMSO-d_6): δ 5.19 (s, 2H, NCH_2); 7.22 (m, 2H, arom); 7.52–7.60 (m, 5H, arom); 7.63 (m, 2H, arom); 7.76–8.01 (m, 6H, arom); 8.16 (s, 1H, CH methylidene); Anal. calcd for $C_{29}H_{19}F_3N_2O_3S$: C, 65.41; H, 3.60; N, 5.26. Found: C, 65.29; H, 3.38; N, 5.01.

*5.1.3.6. 4-{[2-(4-Methoxyphenylimino)-4-oxo-5-(3-phenoxybenzylidene)-3-thiazolidinyl]methyl}benzoic acid (**8a**).* Yield 50%; mp 196–198 °C; ^{1}H NMR ($CDCl_3$): δ 3.86 (s, 3H, OCH_3); 5.22 (s, 2H, NCH_2); 6.91–7.03 (m, 6H, arom); 7.12–7.19 (m, 3H, arom); 7.29–7.36 (m, 4H, arom); 7.60 (m, 2H, arom); 7.70 (s, 1H, CH methylidene); 8.08 (m, 2H, arom); ^{13}C NMR (DMSO-d_6): δ 47.3 (NCH_2); 55.6 (OCH_3); 115.0, 119.7, 119.9, 124.4, 125.1, 127.8, 129.9, 130.1, 130.4, 131.2 (CH arom); 127.9 (C5); 135.4, 140.7, 154.7, 156.1, 157.3, 158.1 (Cq); 166.1, 168.1 (CO); Anal. calcd for $C_{31}H_{24}N_2O_5S$: C, 69.39; H, 4.51; N, 5.22. Found: C, 69.28; H, 4.39; N, 5.34.

*5.1.3.7. 4-{[2-(4-Methoxyphenylimino)-4-oxo-5-(4-phenoxybenzylidene)-3-thiazolidinyl]methyl}benzoic acid (**8b**).* Yield 50%; mp 243–245 °C; ^{1}H NMR ($CDCl_3$): δ 3.83 (s, 3H, OCH_3); 5.23 (s, 2H, NCH_2); 6.93 (m, 5H, arom); 7.00 (m, 2H, arom); 7.04 (m, 2H, arom); 7.36 (m, 2H, arom), 7.43 (m, 2H, arom); 7.62 (m, 2H, arom); 7.75 (s, 1H, CH methylidene); 8.08 (m, 2H, arom); ^{13}C NMR (DMSO-d_6): δ 40.3 (NCH_2); 55.4 (OCH_3); 114.9, 118.6, 119.7, 124.6, 127.8, 129.6, 129.8, 130.2, 130.3, 130.4, 132.2 (CH arom); 119.8 (C5); 127.8, 140.7, 141.2, 149.3, 156.1, 158.7, 158.8 (Cq); 166.0, 168.1 (CO); Anal. calcd for $C_{31}H_{24}N_2O_5S$: 69.39; H, 4.51; N, 5.22. Found: C, 69.45; H, 4.43; N, 5.31.

*5.1.3.8. 4-{[5-(3-Benzyloxybenzylidene)-2-(4-methoxyphenylimino)-4-oxo-3-thiazolidinyl]methyl}benzoic acid (**8c**).* Yield 38%; mp 205–207 °C; ^{1}H NMR ($CDCl_3$): δ 3.84 (s, 3H, OCH_3); 5.08 (s, 2H,

NCH_2); 5.23 (s, 2H, OCH_2); 6.94–7.08 (m, 6H, arom); 7.33–7.39 (m, 7H, arom); 7.62 (m, 2H, arom); 7.73 (s, 1H, CH methylidene); 8.10 (m, 2H, arom); ^{13}C NMR (DMSO-d_6): δ 45.9 (NCH_2); 55.6 (OCH_3); 69.7 (OCH_2); 115.1, 116.7, 117.2, 121.8, 122.1, 122.2, 122.5, 127.9, 128.0, 128.3, 128.8, 130.3 (CH arom); 121.2 (C5); 132.6, 140.8, 157.1, 159.0, 159.4 (Cq); 166.0, 167.4 (CO); Anal. calcd for $C_{32}H_{26}N_2O_5S$: C, 69.80; H, 5.09; N, 4.76. Found: C, 69.69; H, 5.29; N, 4.66.

*5.1.3.9. 4-{[5-(4-Benzyloxybenzylidene)-2-(4-methoxyphenylimino)-4-oxo-3-thiazolidinyl]methyl}benzoic acid (**8d**).* Yield 40%; mp 225–227 °C; ^{1}H NMR ($CDCl_3$): δ 3.84 (s, 3H, OCH_3); 5.10 (s, 2H, NCH_2); 5.22 (s, 2H, OCH_2); 6.94 (m, 4H, arom); 7.01 (m, 2H, arom); 7.40 (m, 7H, arom); 7.61 (m, 2H, arom); 7.73 (s, 1H, CH methylidene); 8.07 (m, 2H, arom); ^{13}C NMR (DMSO-d_6): δ 40.4 (NCH_2); 55.6 (OCH_3); 69.8 (OCH_2); 115.0, 115.9, 126.2, 127.8, 128.7, 129.9, 130.0, 132.2 (CH arom); 118.3 (C5); 126.3, 130.3, 140.8, 141.2, 156.8, 160.1 (Cq); 166.2 (CO); Anal. calcd for $C_{32}H_{26}N_2O_5S$: C, 69.80; H, 5.09; N, 4.76. Found: C, 69.64; H, 5.25; N, 4.59.

*5.1.3.10. 4-{[2-(4-Methoxyphenylimino)-5-(naphthalen-2-ylmethylidene)-4-oxo-3-thiazolidinyl]methyl}benzoic acid (**8e**).* Yield 41%; mp 250–252 °C; ^{1}H NMR (DMSO-d_6): δ 3.75 (s, 3H, OCH_3); 5.19 (s, 2H, NCH_2); 6.98 (s, 4H, arom); 6.98 (m, 4H, arom); 7.49–7.65 (m, 5H, arom); 7.92–8.01 (m, 6H, arom); 8.15 (s, 1H, CH methylidene); Anal. calcd for $C_{29}H_{22}N_2O_4S$: C, 70.43; H, 4.48; N, 5.66. Found: C, 70.27; H, 4.37; N, 5.51.

5.2. Molecular modelling

Docking studies including protein and ligand preparations were carried out using the software GOLD 5 (http://www.ccdc.cam.ac.uk/products/life_sciences/gold/) [65,67] using default parameters (GOLDScore, 100% search efficiency). PDB [61] entries 2QBS [62] (human PTP1B), 5PNT [63] (LMW-PTP IF1) and 1XWW [64] (LMW-PTP IF2) were selected as protein templates. The active site was determined by selecting all residues with any atom within 7 Å from the outside atoms the co-crystallized ligand for 2QBS, and the analogue residues for the other two PDB structures using the sequence alignment and structure overlay functionality of the software tool MOE [68] provided by the Chemical Computing Group (http://www.chemcomp.com/). Docking was performed without any constraints and all compounds were minimized using LigandScout's [66,69,70] general purpose MMFF94 implementation after docking. In order to get the most probable binding poses, a 3D pharmacophore was developed using LigandScout. For 2QBS the co-crystallized ligand was used, for 5PNT and 1XWW analog 3D pharmacophores were created using the docking poses of the most active ligands synthesized in this work. These 3D pharmacophores were then utilized to select the docking poses that formed the basis for the analysis described. LigandScout was also used for visualization and analysis.

5.3. Enzyme section

The complete coding sequences of human IF1, IF2 LMW-PTPs and human PTP1B were cloned in frame with the sequence of the glutathione S-transferase in the pGEX-2T bacterial expression vector. Enzyme expression and purification were achieved in the *Escherichia coli* TB1 strain [71]. Briefly, the recombinant fusion proteins were purified from bacterial lysate using a single step affinity chromatography on glutathione-Sepharose. The solution containing purified fusion proteins was treated with thrombin for 3 h at 37 °C. Then the enzymes were purified from GST and thrombin by gel filtration on Superdex G-75. The purity of protein preparations were analyzed by SDS–polyacrylamide gel electrophoresis according to Laemmli [72]. Recombinant TC-PTP was obtained from New England Biolabs.

5.3.1. Phosphatase assay and inhibition experiments

PTP1B and LMW-PTP assay was carried out at 37 °C using *p*-nitrophenylphosphate as substrate and the final volume was 1 ml. The assay buffer (pH 7.0) contained 0.075 M β,β-dimethylglutarate buffer, 1 mM EDTA and 5 mM dithiothreitol. The reactions were initiated by addition of aliquots of the enzyme preparations and stopped at appropriate times by adding 4 ml of 1 M KOH. The released *p*-nitrophenolate ion was determined by reading the absorbance at 400 nm (ε = 18,000 M^{-1} cm^{-1}). The main kinetic parameters (K_m and V_{max}) were determined by measuring the initial rates at different substrate concentrations. Experimental data were analysed using the Michaelis equation and a non-linear fitting program FigSys [73]. Inhibition constants were determined measuring initial hydrolysis rates at differing substrate and inhibitor concentrations. The apparent K_m values measured at the various inhibitor concentrations were plotted against concentration of the inhibitor to calculate the K_i values. All measurements of initial rate were carried out in triplicate. For each inhibitor, IC_{50} was determined by measuring the initial hydrolysis rate under fixed *p*-nitrophenylphosphate concentration, equal to the K_m value of each tested PTP. Data were fitted to the following equation using the FigSys program:

$$y = \frac{\text{Max} - \text{Min}}{1 + \left(\frac{x}{IC_{50}}\right)^{\text{slope}}} + \text{Min}$$

where $y = v_i/v_o$, i.e. the ratio between the activity measured in the presence of the inhibitor (v_i) and the activity of the control without the inhibitor (v_o). The parameter "*x*" is the inhibitor concentration.

To verify if compounds **7a**–**e** and **8a**–**e** were reversible inhibitors, appropriate aliquots of PTP1B were incubated in the presence of at least 25-fold molar excess of inhibitor for 1 h at 37 °C. Control experiments were performed adding DMSO instead of inhibitor. After this interval time, the enzyme solutions were diluted 200-fold and the residual enzyme activity was assayed.

The assay of TC-PTP activity was performed as follows: an appropriate aliquot of enzyme (0.02 μg) was diluted to 0.75 ml with the same assay buffer used for the other PTPs, containing *p*-nitrophenylphosphate at the final concentration 2.8 mM (a value corresponding to that of the enzyme K_m). After the appropriate incubation time, reactions were stopped by adding 0.25 ml of 0.4 M KOH. The released *p*-nitrophenolate ion was measured reading the absorbance at 400 nm. The IC_{50} values were determined as described above.

5.3.2. Cellular assays

C2C12 cells were obtained from the European Collection of Cell Cultures (Salisbury, UK). Assays were carried out using differentiating mouse C2C12 myoblasts which constitutively express both PTP1B and IR. Cells were grown in DMEM, supplemented with 10% FBS, 2 mM L-glutamine, 100 U/ml penicillin, and 100 μg/ml streptomycin at 37 °C in 5% CO_2 humidified atmosphere. To induce differentiation, the medium of 90% subconfluent cells was replaced by DMEM supplemented with 2% horse serum, and cells were incubated at 37 °C. After 2 days, the medium was replaced by fresh differentiation medium, and cells were incubated for additional 2 days at the same conditions. The obtained myotubes were starved for 20 h before experiments. Compounds **7a**–**e** and **8a**–**e** (25 μM final concentration) or DMSO (1.2% final concentration) were added to the culture medium and the cells were incubated for 90 min at 37 °C. The positive control with insulin (10 nM final concentration)

was carried out incubating cells for 30 min a 37 °C. The cells were then lysed with SDS Laemmly sample buffer and analyzed by SDS-PAGE and Western Blot using both anti-phosphorylated insulin receptor and anti-actin antibodies (Santa Cruz Biotechnology Inc.).

To perform the cytotoxicity assays, DMEM was supplemented with MTT (0.5 mg/ml final concentration) and then myotubes were incubated at 37 °C. After 2 h, the medium was removed and cells were lysed with DMSO. The absorption levels of formazan were read at 570 nm.

To determine glucose uptake, C2C12 cells were seeded in 24-well plates, differentiated as described above, and serum-starved for 20 h. Then the myotubes were treated with compounds **7a**–**e** and **8a**–**e** (25 μM final concentration) or 1.2% DMSO for 90 min. The positive control with insulin (10 nM final concentration) was carried out incubating cells for 30 min a 37 °C.

Glucose transport was assayed as follows: after inhibitor or other treatments, 0.1 μCi of 2-deoxy-D-1,2-[^{3}H]-glucose (20 Ci/mmol) in Ringer–Hepes buffer was added to each well and glucose uptake was allowed at 37 °C for 15 min. Cells were subsequently washed with cold PBS and lysed in 0.2 M NaOH. Aliquots of the lysates were counted with a β-scintillation counter, and data were normalized against protein concentration.

Acknowledgements

Work supported in part by the 'Ente Cassa di Risparmio di Firenze' and by University of Messina.

Appendix. Supplementary material

Supplementary material associated with this article can be found, in the online version, at doi:10.1016/j.ejmech.2012.02.012.

References

[1] A. Alonso, J. Sasin, N. Bottini, I. Friedberg, A. Osterman, A. Godzik, T. Hunter, J. Dixon, T. Mustelin, Cell 117 (2004) 699–711.
[2] T. Hunter, Cell 100 (2000) 113–127.
[3] B.G. Neel, N.K. Tonks, Curr. Opin. Cell Biol. 9 (1997) 193–204.
[4] N.K. Tonks, Nat. Rev. Mol. Cell Biol. 7 (2006) 833–846.
[5] S. Koren, I.G. Fantus, Best Pract. Res. Cl. En. 21 (2007) 621–640.
[6] N. Dubè, M.L. Tremblay, Biochim. Biophys. Acta 1754 (2005) 108–117.
[7] A. Ostman, C. Hellberg, F.D. Böhmer, Nat. Rev. Cancer 6 (2006) 307–320.
[8] V.V. Vintonyak, A.P. Antonchick, D. Rauh, H. Waldmann, Curr. Opin. Chem. Biol. 13 (2009) 272–283.
[9] J. Zang, P.L. Yang, N.S. Gray, Nat. Rev. Cancer 9 (2009) 28–39.
[10] V.R.H. Huijsduijnen, A. Bombrum, D. Swinnen, Drug Discov. Today 7 (2002) 1013–1019.
[11] M.A.T. Blaskovich, Cur. Med. Chem. 16 (2009) 2095–2176.
[12] P. Heneberg, Curr. Med. Chem. 16 (2009) 706–733.
[13] V.V. Vintonyak, H. Waldmann, D. Rauh, Bioorg. Med. Chem. 19 (2011) 2145–2155.
[14] M. Elchebly, P. Payette, E. Michaliszyn, W. Cromlish, S. Collins, A.L. Loy, D. Normandin, A. Cheng, J. Himms-Hagen, C. Chan, C. Ramachandran, M.J. Gresser, M.L. Tremblay, B.P. Kennedy, Science 283 (1999) 1544–1548.
[15] L.D. Klaman, O. Boss, O.D. Peroni, J.K. Kim, J.L. Martino, J.M. Zabolotny, N. Moghal, M. Lubkin, Y.B. Kim, A.H. Sharpe, A. Stricker-Krongrad, G.I. Shulman, B.G. Neel, B.B. Kahn, Mol. Cell. Biol. 20 (2000) 5479–5489.
[16] N.K. Tonks, FEBS Lett. 546 (2003) 140–148.
[17] G. Liu, Curr. Opin. Mol. Ther. 6 (2004) 331–336.
[18] A. Cheng, N. Uetani, P.D. Simoncic, V.P. Chaubey, A. Lee-Loy, J. McGlade, B.P. Kennedy, M.L. Tremblay, Dev. Cell 2 (2002) 497–503.
[19] J.M. Zabolotny, K.K. Bence-Hanulec, A. Stricker-Krongrad, F. Haj, Y. Wang, Y. Minokoshi, Y.B. Kim, J.K. Elmquist, L.A. Tartaglia, B.B. Kahn, B.G. Neel, Dev. Cell 2 (2002) 489–495.
[20] T. Tiganis, A.M. Bennett, Biochem. J. 402 (2007) 1–15.
[21] K.A. Kenner, E. Anyanwu, J.M. Olefsky, J. Kusari, J. Biol. Chem. 33 (1996) 19810–19816.
[22] B.A. Zinker, C.M. Rondinone, J.M. Trevillyan, R.J. Gum, J.E. Clampit, J.F. Waring, N. Xie, D. Wilcox, P. Jacobson, L. Frost, P.E. Kroeger, R.M. Reilly, S. Koterski, T.J. Opgenorth, R.G. Ulrich, S. Crosby, M. Butler, S.F. Murray, R.A. McKay, S. Bhanot, B.P. Monia, M.R. Jirousek, Proc. Natl. Acad. Sci. USA 17 (2002) 11357–11362.
[23] M.M. Swarbrick, P.J. Havel, A.A. Levin, A.A. Bremer, K.L. Stanhope, M. Butler, S.L. Booten, J.L. Graham, R.A. Mckay, S.F. Murray, L.M. Watts, B.P. Monia, S. Bhanot, Endocrinology 150 (2009) 1670–1679.
[24] T.O. Johnson, J. Ermolieff, M.R. Jirousek, Nat. Rev. Drug Discov. 1 (2002) 696–709.
[25] B.P. Montalibet, B.P. Kennedy, Drug Discov. Today Ther. Strateg. 2 (2005) 129–135.
[26] A.M. Hennige, N. Stefan, K. Kapp, R. Lehmann, C. Weigert, A. Beck, K. Moeschel, J. Mushack, E. Schleicher, H.-U. Haring, FASEB J. 20 (2006) E381–E389.
[27] G. Sesti, Best Pract. Res. Cl. En. 20 (2006) 665–679.
[28] J.E. Shaw, R.A. Sicree, P.Z. Zimmet, Diabetes Res. Clin. Pract. 87 (2010) 4–14.
[29] A.P. Combs, J. Med. Chem. 53 (2010) 2333–2344.
[30] S. Lee, Q. Wang, Med. Res. Rev. 27 (2007) 553–573.
[31] S. Zhang, Z.Y. Zhang, Drug Discov. Today 12 (2007) 373–381.
[32] D.V. Erbe, S. Wang, Y.L. Zhang, K. Harding, L. Kung, M. Tam, L. Stolz, Y. Xing, S. Furey, A. Qadri, L.D. Klaman, J.F. Tobin, Mol. Pharmacol. 67 (2005) 69–77.
[33] N. Takahashi, Y. Qi, H.R. Patel, R.S. Ahima, J. Hepatol. 41 (2004) 391–398.
[34] K.A. Lantz, S.G. Hart, S.L. Planey, M.F. Roitman, I.A. Ruiz-White, H.R. Wolfe, M.P. McLane, Obesity 18 (2010) 1516–1523.
[35] S.K. Pandey, X.X. Yu, L.M. Watts, M.D. Michael, K.W. Sloop, A.R. Rivard, T.A. Leedom, V.P. Manchem, L. Samadzadeh, R.A. McKay, B.P. Monia, S. Bhanot, J. Biol. Chem. 282 (2007) 14291–14298.
[36] P. Chiarugi, P. Cirri, F. Marra, G. Raugei, G. Camici, G. Manao, G. Ramponi, Biochem. Biophys. Res. Commun. 238 (1997) 676–682.
[37] M.L. Taddei, P. Chiarugi, P. Cirri, D. Talini, G. Camici, G. Manao, G. Raugei, G. Ramponi, Biochem. Biophys. Res. Commun. 270 (2000) 564–569.
[38] R. Maccari, R. Ottanà, J. Med. Chem. 55 (2012) 2–22.
[39] L.F. Iversen, K.B. Møller, A.K. Pedersen, G.H. Peters, A.S. Petersen, H.S. Andersen, S. Branner, S.B. Mortensen, N.P.H. Møller, J. Biol. Chem. 277 (2002) 19982–19990.
[40] A. Bourdeau, N. Dubé, M.L. Tremblay, Curr. Opin. Cell Biol. 17 (2005) 203–209.
[41] K.M. Heinon, K.M. Heinonen, F.P. Nestel, E.W. Newell, G. Charette, T.A. Seemayer, M.L. Tremblay, W.S. Lapp, Blood 103 (2004) 3457–3464.
[42] S. Galic, C. Hauser, B.B. Kahn, F.G. Haj, B.G. Neel, M.K. Tonks, T. Tiganis, Mol. Cell. Biol. 25 (2005) 819–829.
[43] S. Galic, M. Klingler-Hoffmann, M.T. Fodero-Tavoletti, M.A. Puryer, T.-C. Meng, M.K. Tonks, T. Tiganis, Mol. Cell. Biol. 23 (2003) 2096–2108.
[44] A. Fukushima, K. Loh, S. Galic, B. Fam, B. Shields, F. Wiede, M.L. Tremblay, M.J. Watt, S. Andrikopoulos, T. Tiganis, Diabetes 59 (2010) 1906–1914.
[45] K. Loh, A. Fukushima, X. Zhang, S. Galic, D. Briggs, P.J. Enriori, S. Simonds, F. Wiede, A. Reichenbach, C. Hauser, N.A. Sims, K.K. Bence, S. Zhang, Z.-Y. Zhang, B. Kahn, B.G. Neel, Z.B. Andrews, M.A. Cowley, T. Tiganis, Cell Metab. 14 (2011) 684–698.
[46] A.J. Nichols, R.D. Mashal, B. Balkan, Drug Develop. Res. 67 (2006) 559–566.
[47] C. Li, X.-P. He, Y.-J. Zhang, Z. Li, L.-X. Gao, X.-X. Shi, J. Xie, J. Li, G.-R. Chen, Y. Tang, Eur. J. Med. Chem. 46 (2011) 4212–4218.
[48] L. Tabernero, A.R. Aricescu, E.Y. Jones, S.E. Szedlacsek, FEBS J. 275 (2008) 867–882.
[49] G. Scapin, S.B. Patel, J.W. Becker, Q. Wang, C. Desponts, D. Waddleton, K. Skorey, W. Cromlish, C. Bayly, M. Therien, J.Y. Gauthier, C.S. Li, C.K. Lau, C. Ramachandran, B.P. Kennedy, E. Asante-Appiah, Biochemistry 42 (2003) 11451–11459.
[50] Y.A. Puius, Y. Zhao, M. Sullivan, D.S. Lawrence, S.C. Almo, Z.Y. Zhang, Proc. Natl. Acad. Sci. USA 94 (1997) 13420–13425.
[51] P. Cirri, T. Fiaschi, P. Chiarugi, G. Camici, G. Manao, G. Raugei, G. Ramponi, J. Biol. Chem. 271 (1996) 2604–2607.
[52] A.P.R. Zabell, A.D. Schroff, B.E. Bain, R.L. Van Etten, O. Wiest, C.V. Stauffacher, J. Biol. Chem. 281 (2006) 2604–2607.
[53] R. Maccari, P. Paoli, R. Ottanà, M. Jacomelli, R. Ciurleo, G. Manao, T. Steindl, T. Langer, M.G. Vigorita, G. Camici, Bioorg. Med. Chem. 15 (2007) 5137–5149.
[54] R. Maccari, R. Ottanà, R. Ciurleo, P. Paoli, G. Manao, G. Camici, C. Laggner, T. Langer, ChemMedChem 4 (2009) 957–962.
[55] R. Ottanà, R. Maccari, R. Ciurleo, P. Paoli, M. Jacomelli, G. Manao, G. Camici, C. Laggner, T. Langer, Bioorg. Med. Chem. 17 (2009) 1928–1937.
[56] R. Ottanà, R. Maccari, M.L. Barreca, G. Bruno, A. Rotondo, A. Rossi, G. Chiricosta, R. Di Paola, L. Saubetin, S. Cuzzocrea, M.G. Vigorita, Bioorg. Med. Chem. 13 (2005) 4243–4252.
[57] G. Bruno, L. Costantino, C. Curinga, R. Maccari, F. Monforte, F. Nicolò, R. Ottanà, M.G. Vigorita, Bioorg. Med. Chem. 10 (2002) 1077–1084.
[58] Y. Momose, K. Meguro, H. Ikeda, C. Hatanaka, S. Oi, T. Sohada, Chem. Pharm. Bull. 39 (1991) 1440–1445.
[59] T. Ispida, Y. In, M. Inoue, C. Tanaka, N. Hamanaka, J. Chem. Soc. Perkin Trans. 2 (1990) 1085–1091.
[60] U. Iannaccone, A. Bergamaschi, A. Magrini, G. Marino, N. Bottini, P. Lucarelli, E. Bottini, F. Gloria-Bottini, Metab. Clin. Exp. 54 (2005) 891–894.
[61] H.L. Berman, J. Westbrook, Z. Feng, G. Gilliland, T.N. Bhat, H. Weissig, I.N. Shindyalov, P.E. Bourne, Nucl. Acids Res. 28 (2000) 235–242.
[62] D.P. Wilson, Z.-K. Wan, W.-X. Xu, S.J. Kirincich, B.C. Follows, D. Joseph-McCarthy, K. Foreman, A. Moretto, J. Wu, M. Zhu, E. Binnun, Y.-L. Zhang, M. Tam, D.V. Erbe, J. Tobin, X. Xu, L. Leung, A. Shilling, S.Y. Tam, T.S. Mansour, J. Lee, J. Med. Chem. 20 (2007) 4681–4698.
[63] M. Zhang, C.V. Stauffacher, D. Lin, R.L. Van Etten, J. Biol. Chem. 273 (1998) 21714–21720.
[64] A.P.R. Zabell, A.D. Schroff Jr., B.E. Bain, R.L. Van Etten, O. Wiest, C.V. Stauffacher, J. Biol. Chem. 281 (2006) 6520–6527.

[65] G. Jones, P. Willett, R.C. Glen, J. Mol. Biol. 245 (1995) 43–53.
[66] G. Wolber, T. Langer, J. Chem. Inf. Model. 45 (2005) 160–169.
[67] G. Jones, P. Willett, R.C. Glen, A.R. Leach, R. Taylor, J. Mol. Biol. 267 (1997) 727–748.
[68] Molecular operating environment (MOE), version 2010.20, Chemical Computing group, 1010 Sherbrooke St. W, Suite 910, Montreal, Quebec, Canada.
[69] T. Seidel, G. Ibis, F. Bendix, G. Wolber, Drug Discov. Today Tecnologies 7 (2010) e221–e228.
[70] G. Wolber, A.A. Dornhofer, T. Langer, J. Comput. Aid. Mol. Des 20 (2006) 773–788.
[71] R. Marzocchini, M. Bucciantini, M. Stefani, N. Taddei, M.G.M.M. Thunnissen, P. Nordlund, G. Ramponi, FEBS Lett. 426 (1998) 52–56.
[72] U.K. Laemmli, Nature 227 (1970) 680–685.
[73] FigSys® 2003, A Graphing, Charting and Data Analysis Software Package, is produced by BIOSOFT®, 2D Dolphin Way, Stapleford Cambridge, CB2 5DW, UK.